

Y₂O₃:Eu and the Mössbauer isomer shift coefficient of Eu compounds from *ab-initio* simulations

Arkadiy Davydov^{1,2} , Antonio Sanna^{3,*}  and Giorgio Concas⁴ 

¹ Department of Physics, University of Zurich, Winterthurerstrasse 190, 8057 Zurich, Switzerland

² Scientific Computing Research Technology Platform, University of Warwick, Zeeman Building, CV4 7AL Coventry, United Kingdom

³ Max-Planck-Institut für Mikrostrukturphysik, Weinberg 2, D-06120 Halle, Germany

⁴ Department of Physics, University of Cagliari, S.P. Monserrato-Sestu km 0, 700, I-09042 Monserrato (CA), Italy

E-mail: sanna@mpi-halle.mpg.de

Received 24 August 2021, revised 29 October 2021

Accepted for publication 9 November 2021

Published 29 November 2021



Abstract

We report on a full potential density functional theory characterization of Y₂O₃ upon Eu doping on the two inequivalent crystallographic sites *24d* and *8b*. We analyze local structural relaxation, electronic properties and the relative stability of the two sites. The simulations are used to extract the contact charge density at the Eu nucleus. Then we construct the experimental isomer shift (IS) versus contact charge density calibration curve, by considering an ample set of Eu compounds: EuF₃, EuO, EuF₂, EuS, EuSe, EuTe, EuPd₃ and the Eu metal. The, expected, linear dependence has a slope of $\alpha = 0.054 \text{ mm s}^{-1} \text{ \AA}^{-3}$, which corresponds to nuclear expansion parameter $\Delta R/R = 6.0 \times 10^{-5}$. α allows to obtain an unbiased and accurate estimation of the IS for any Eu compound. We test this approach on two mixed-valence compounds Eu₃S₄ and Eu₂SiN₃, and use it to predict the Y₂O₃ : Eu IS with the result $+1.04 \text{ mm s}^{-1}$ at the *24d* site and $+1.00 \text{ mm s}^{-1}$ at the *8b* site.

Keywords: Eu, Y₂O₃:Eu, Mössbauer isomer shift, DFT simulations

(Some figures may appear in colour only in the online journal)


Yttrium sesquioxide doped with lanthanide ions are technologically relevant materials with a broad set of applications, especially owing to their luminescence properties [1]. In particular, Eu³⁺ doped cubic Y₂O₃ is one of the best red emitting phosphors [2, 3]. In such doped system is of extreme importance how the rare earth ions distribute. Apart from a possible clusterization, the Eu ions can go in two symmetrically distinct sites (with *8b* or *24d* Wyckoff position in the *Ia3* space group). A theoretical study based on atomistic

simulations, finds a preferential occupation of the *8b* site [4]. Magnetic susceptibility experiments observe a preferential occupation of the *24d* site [5, 6]. On the contrary, x-ray diffraction [7] suggest a random distribution of Eu, confirmed by Mössbauer spectroscopic studies [8].

Mössbauer spectroscopy is a powerful instrument of characterization because it probes directly at the Eu site, therefore giving information on the local chemical environment. However the Mössbauer signal needs to be fitted in order to extract the valuable physical information. When dealing with multiple Eu sites with unknown occupation such fitting procedure is not straightforward and involves some biases.

In this paper we present an approach to use *ab initio* density functional theory (DFT) simulations in connection and as support to Mössbauer spectroscopy. The theoretical approach

* Author to whom any correspondence should be addressed.

 Original content from this work may be used under the terms of the [Creative Commons Attribution 4.0 licence](https://creativecommons.org/licenses/by/4.0/). Any further distribution of this work must maintain attribution to the author(s) and the title of the work, journal citation and DOI.

is introduced in section 1. In section 2 we provide an accurate theoretical characterization of Eu doping in Y_2O_3 and the relative energetics. Simulations allow to extract the contact charge density which is the electronic density at the Eu nucleus. As a second step we construct an empirical map between the contact charge density and the isomer shift (IS) as measured in Mössbauer spectroscopy. The map (discussed in section 3) is built by performing DFT simulations on a set of Eu compounds for which the IS is experimentally known. The materials in this set are chosen to have Eu in different coordination and chemical status and such that there is one single fully occupied Eu Wyckoff position, which makes the experimental estimation of the IS more reliable. Last (section 3) we show that the map can be used to obtain the IS of other Eu compounds, like those where Eu has multiple valences. The map is finally used to predict the ISs for $\text{Y}_2\text{O}_3 : \text{Eu}$.

1. Methods and numerical parameters

We perform density functional [9, 10] theory simulations within the all-electron full-potential linearised augmented-*plane*wave (FP-LAPW) method [11], as implemented in the *elk* [12] code. Exchange correlation (*xc*) effects are included in the local spin density approximation (LSDA) and the LSDA + *U* method, where a Hubbard *U* correction [13] is applied to the Eu *f*-shell. We adopt $U = 7$ eV and $J = 0.75$ eV, as validated [14] for the isostructural Eu_2O_3 compound; nevertheless we will discuss the impact of this choice for the results obtained in this work. All calculations include spin-orbit interactions and allow for arbitrary non-collinear spin ordering.

The Brillouin zone integration is performed in a $2 \times 2 \times 2k$ -point Monkhorst Pack mesh [15]. The maximum length of the \mathbf{G} expansion is fixed by the $R_{\text{MT}} \times |\mathbf{G} + \mathbf{k}|$ parameter set to 7. R_{MT} is the smallest among the muffin-tin radii, which are 2.2, 2.2 and 1.6 Bohr, respectively for Eu, Y and O.

An Eu nuclear radius of 6.4 fm is used to compute the Mössbauer contact charge density, and was derived [16] from the relation $R = 1.2A^{1/3}$ fm, where *A*, the mass number of the Mössbauer active Europium, is taken to be 151.

Numerical results were obtained by fully minimizing internal forces, while Bravais lattice parameters are linearly interpolated, as a function of Eu content, from those of the parent compounds Y_2O_3 and Eu_2O_3 (10.602 and 10.859 Å respectively [17]).

All other systems studied in this work (listed in the text and used to obtain figure 3) have been studied at the experimental lattice positions and using the same computational parameters and methods as above, as well as a similarly dense reciprocal space discretization.

2. Structural and electronic properties of $\text{Y}_2\text{O}_3 : \text{Eu}$

The host compound Y_2O_3 crystallises in the cubic bixbyte structure with $T_h^7 (Ia\bar{3})$ symmetry, its primitive cell is body centered and composed by 10 formula units [18]. An important aspect is that there are two symmetry-inequivalent Y sites:

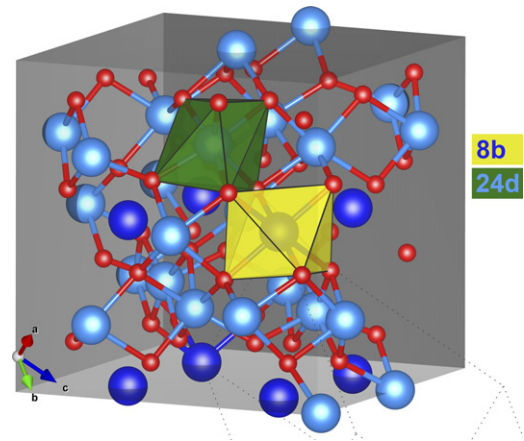


Figure 1. The crystal structure of the Y_2O_3 oxide. Dark blue balls are Y-atoms in $8b$ position (S_6 symmetry—the coordination octahedra is shown in yellow). Light blue balls are Y-atoms in $24d$ position (C_2 symmetry—the coordination polyhedra is shown in green). Red balls are oxygen atoms.

the $8b$ site, has S_6 symmetry and hosts 1/4 of Y atoms; the $24d$ site has the lower C_2 symmetry and hosts the remaining 3/4 of the Yttrium. The structure is shown in figure 1. The local symmetry of the $8b$ and $24d$ sites is highlighted showing the respective oxygen coordination polyhedra. From the electronic point of view Y_2O_3 is a non-magnetic insulator, with an experimental band gap of 6 eV. The Kohn–Sham DFT approximation, as expected [19], gives a smaller value which is 4.3 eV. An accurate numerical estimation can be usually achieved by many body perturbation theory in the G_0W_0 approximation for the electronic self-energy [20, 21]; however the bixbyte structure is too large and complicated for this kind of calculations. The computed density of states is shown in figure 2(a). As a validation test we have simulated the optical absorption spectrum and compared with available experimental data [22]. For a fair comparison we have included a 1.86 eV scissor correction to the conduction band. The agreement (see figure 2(b)) in the basic RPA approximation (neglecting *xc* effects on the response function) is fair as it reproduces the main absorption peak between 5 and 15 eV. A second structure is observed at about 30 eV which experimentally seems to be broader and merge with the main peak. The inclusion of *xc* contribution within the Bootstrap approximation [23–25] for f_{xc} improves the shape of the main peak, and especially the form of its near-gap part (see inset in figure 2(b)).

An Y to Eu substitution can be obtained at any level up to the completely substituted system Eu_2O_3 . However the most relevant regime is the low doping one, with $\sim 5\%$ of Eu, since this corresponds to the maximal optical efficiency [26]. In simulations we consider a low Eu doping limit of the Y_2O_3 crystal, and assume no interaction among Europium ions. Owing to the large unit cell size this can be simulated by the replacement of one single Y per cell. This $\text{Eu} \rightarrow \text{Y}$ substitution causes a local expansion of the O coordination polyhedra, consistently with the larger Eu ionic size. The modified bonding lengths are reported in table 1. Accurate total energy estimation shows that the $24d$ crystal site is more stable than the $8b$ by

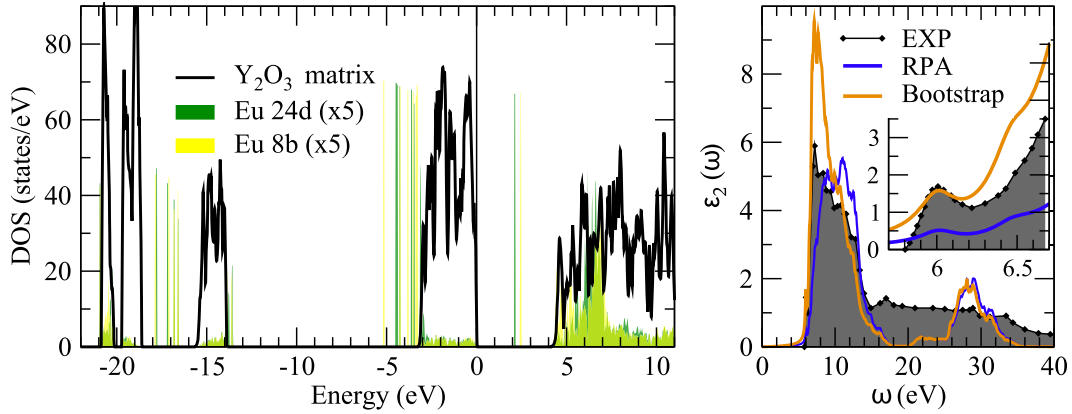


Figure 2. Left: density of electronic states of Y₂O₃ (black) and contribution from Eu impurities in the 24*d* (green) and 8*b* (yellow) sites. Right: the RPA and bootstrap-TDDFT [23, 25] absorption spectra for Y₂O₃ in comparison with the experimental results from reference [22].

Table 1. Eu–O nearest neighbor distances and their percentual changes with respect to the unsubstituted Y₂O₃ system.

	Eu(8 <i>b</i>)		Eu(24 <i>d</i>)	
	Unrelaxed (Å)	Relaxed (change, %)	Unrelaxed (Å)	Relaxed (change, %)
O ¹	2.285	1.86	2.325	1.57
O ²	2.285	2.13	2.325	1.68
O ³	2.285	1.73	2.279	1.00
O ⁴	2.285	2.17	2.279	1.07
O ⁵	2.285	1.80	2.251	2.77
O ⁶	2.285	2.11	2.251	2.63

$\Delta_E \simeq 90$ meV. This relatively high energy difference (corresponding to ~ 1050 K), indicates that the 8*b* population should be lower than the 24*d*. A quantitative estimation can be done by using Boltzmann statistic and assuming that occupations to be frozen as the crystal is formed (~ 1000 K); in this case then the occupation factor of the 24*d* sites should be of about 0.73 (against the 0.5 expected for $\Delta_E = 0$). It should be possible to observe this difference; however experiments seem to give contrasting results [5, 6, 8].

The value of U significantly affects the relative stability of the two sites. At $U = 3$ we compute that Δ_E reduces to zero. But in the range of reasonable U values, which for f -electrons is between 6 and 8 eV, Δ_E ranges in the interval 77–108 meV. This corresponds to a small thermal occupation error-bar of ± 0.04 around the occupation population factor of 0.73, supporting the reliability of our numerical estimation. Such U dependence can be accessed only via the ab-initio calculations and is missing in the classical force fields based scheme [4], which predicted the preferable 8*b* population.

The magnetic quantization axis of the Eu ions is the same as for the Eu₂O₃, being along the (111) cubic direction for the 8*b* site and along the 100 for the 24*d* site. In simulations we obtain \mathbf{L} , \mathbf{S} and \mathbf{J} to be $1.63 \mu_B$, $2.78 \mu_B$ and $1.15 \mu_B$ for Eu in the 8*b* site; $2.38 \mu_B$, $2.46 \mu_B$, $0.07 \mu_B$ in the 24*d* site, with a total magnetic moment not completely quenched. This aspect in spin density functional theory (SDFT) results has been already observed and discussed in pure Eu₂O₃ [14].

We will now consider in detail the Mössbauer properties of the Eu ion in the two crystallographic sites.

3. Isomer shift of Y₂O₃:Eu and other Europium compounds

The ¹⁵¹Eu Mössbauer spectroscopy measures the impact of the electronic configuration on the nuclear transition levels. The leading effects are: IS, a change in the absorption energy [27] due to the presence of electronic charge (called contact charge density: ρ_0) inside the nuclear volume; the Zeeman splitting induced by the electronic magnetic moment; and the quadrupole interactions, related to the symmetry breaking effect of the crystal field. The Zeeman splitting is not present in Y₂O₃ : Eu due to the paramagnetism of the system, while quadrupole effects are negligible for the 8*b* site and non-negligible for the 24*d* site [8]. In this work we will focus on the IS, as it carries important information on the site distribution and the bond character of the compounds. For example starting with the configuration of Eu³⁺4*f*⁶: if we add a 6*s* electron, the IS increases, while if we add a 4*f* electron, the IS decreases due to the screening effect [28]. On the other hand, there is a very small increase if a 6*p* is added and a very small decrease if a 5*d* is added, always due to a small screening effect [28].

If one assumes a homogeneous nuclear model, the IS (with respect to the source material), is bound to the contact charge density by the relation:

$$IS = \alpha(\rho_0 - \rho_0^S) \quad (1)$$

where ρ_0 and ρ_0^S are the contact charge density of the compound and of the radioactive source respectively and α is a proportionality coefficient. α is given by:

$$\alpha = (4\pi/5)e^2ZR^2(\Delta R/R) \quad (2)$$

where e is the electron charge, Z is the atomic number, R is the nuclear radius in the ground state and ΔR is the variation between the radius of the excited state (nuclear spin $I = 7/2$) and the radius of the ground state (nuclear spin $I = 5/2$). We aim at determining the coefficient α . This will be done

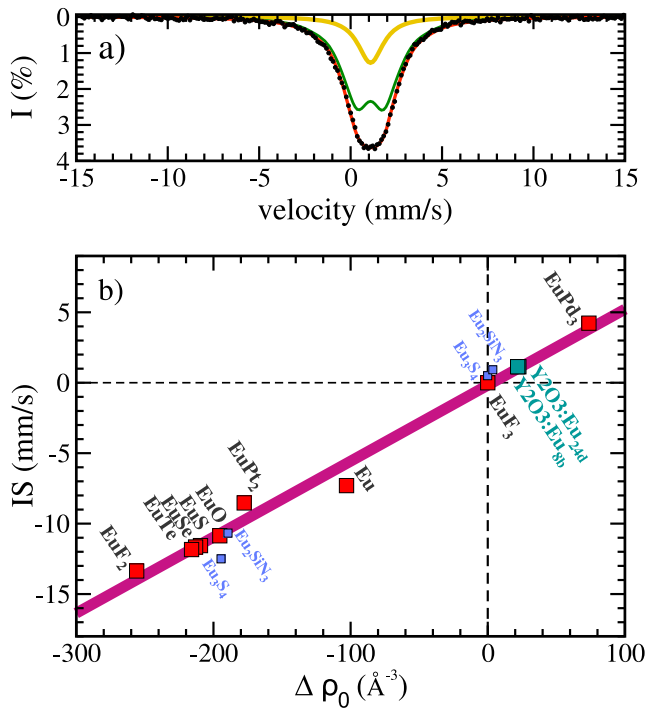


Figure 3. Top: experimental Mössbauer spectrum of $\text{Y}_2\text{O}_3 : \text{Eu}$ reproduced from reference [8]; black dots are the Mössbauer data of a bulk sample. Red is the total fitting curve, green and yellow are the fitted $24d$ and $8b$ components. Bottom: experimental isomer shifts [28, 29] (IS) versus simulated contact charge density ($\Delta\rho_0$) with respect to the EuF_3 compound. Red squares indicate the Eu compounds used to obtain the linear fit (pink line). Violet and blue points are validation points, which are not used for the fit as refer to compounds with more than one Wyckoff Eu site.

by means of first principle calculations of the contact charge density on several Eu compounds. Therefore, we can obtain the nuclear parameter $\Delta R/R$ not by taking a single measure of IS, but by using a fit of IS vs $\Delta\rho_0$ with several measures of IS.

As usual in the Mössbauer spectroscopy of ^{151}Eu , the value of IS is expressed with respect to a reference material which is EuF_3 . Similarly, we will refer to EuF_3 the contact charge density as well, by defining $\Delta\rho_0 := \rho_0 - \rho_0^{\text{EuF}_3}$. This will minimize the effect of theoretical errors, computational parameters and chosen numerical approach.

The proportionality constant α between $\Delta\rho_0$ and the experimental IS can then be obtained from a set of experiments and simulations, and we use the occasion of this work on $\text{Y}_2\text{O}_3 : \text{Eu}$ to compute it. To this end we have considered, beyond EuF_3 seven other Eu compounds, chosen in a broad valence range: EuO , EuF_2 , EuS , EuSe , EuTe , EuPd_3 and the Eu metal. For all of which the IS is known from the literature [16, 28, 29], and we can simulate the contact charge. The results are collected in figure 3.

The linear dependence is quite evident and allows for an accurate estimate of $\alpha = 0.054 \text{ mm s}^{-1} \text{ \AA}^{-3}$. By using this value of α and equation (2), we can calculate the nuclear parameter $\Delta R/R$. In order to do this, it is necessary to consider that the velocity of 1 mm s^{-1} is actually the energy Doppler shift caused by an object which moves at 1 mm s^{-1} ;

this converts to $1.151 \times 10^{-19} \text{ erg}$, obtained by using the energy of the transition (21.54 keV) and the expression of the relativistic longitudinal Doppler effect [30]; the final results is $\Delta R/R = 6.0 \times 10^{-5}$. It is worth to point out that while the results shown in this work are based on the $\text{LDA} + U$, the $\text{GGA} + U$ approach leads to very similar values for the contact charge densities and to the very same value of $\alpha = 0.054 \text{ mm s}^{-1} \text{ \AA}^{-3}$. Moreover our results do not depend critically on the chosen U parameter, as soon the value is physically reasonable.

Using the fitted curve the IS of $\text{Y}_2\text{O}_3 : \text{Eu}$ (or any experimentally unknown Eu compound) can be directly computed from the simulation of ρ_0 . We obtain $+1.045$ for the $24d$ site and $+1.000$ for the $8b$ site. The IS difference of 0.045 mm s^{-1} is small and difficult to observe in experiments without relying on an fitting procedure. The experimental data of a bulk sample, fitted with two components with the constraint of equal IS, give $\text{IS} = 1.14 \text{ mm s}^{-1}$ [8], in good agreement with the calculated value. On the other hand a measure on a nanocrystalline sample fitted allowing for two different ISs at the two sites, gives values of 0.97 mm s^{-1} for the $24d$ site and 1.23 mm s^{-1} for the $8b$ site [31], compatible with the calculated IS.

As a test on the $\text{IS} - \Delta\rho_0$ relation and our estimation for α we consider two mixed-valence europium compounds: Eu_3S_4 and Eu_2SiN_3 . The Eu_3S_4 sulfide crystallizes in the $I42d$ space group and Eu occupies the $4a$ and $8d$ Wyckoff positions. In our SDFT simulations only $4a$ sites are magnetically ordered while $8d$ are non-magnetic, in agreement with previous studies [32]. At the two sites we obtain $\Delta\rho_0 = -194.5 \text{ \AA}^{-3}$ and $\Delta\rho_0 = -0.08 \text{ \AA}^{-3}$ respectively. Using the relation $\text{IS} = \alpha\Delta\rho_0$ we derive the respective ISs of -10.5 mm s^{-1} and 0.0 mm s^{-1} , in excellent agreement with the experimental estimations [33] of -12.5 mm s^{-1} and $+0.5 \text{ mm s}^{-1}$. The Eu_2SiN_3 compound has the $Cmce$ space group with Eu atoms in two inequivalent $8f$ positions. At the two sites we obtain $\Delta\rho_0 = -189.4 \text{ \AA}^{-3}$ and $\Delta\rho_0 = +3.7 \text{ \AA}^{-3}$ respectively, corresponding to the $\text{IS} = -10.2 \text{ mm s}^{-1}$ and $+0.2 \text{ mm s}^{-1}$, to be compared with the experimental [34] values -10.67 mm s^{-1} and $+0.92 \text{ mm s}^{-1}$.

4. Conclusions

We have presented full-potential DFT characterization of Y_2O_3 upon Eu doping on the two inequivalent crystallographic sites $24d$ and $8b$. Total energy results show that the $24d$ sites are expected with an occupation probability of about 0.73, therefore $\sim 90\%$ of Eu atoms should be hosted in this crystallographic environment.

We propose an approach to determine the Mössbauer IS from the knowledge of the contact charge density and the universal relation between these. Such relation is constructed by considering a broad set of Eu systems (EuF_3 , EuO , EuF_2 , EuS , EuSe , EuTe , EuPd_3 , Eu), and performing a linear fitting of the experimental IS versus the simulated contact charge for which we obtain a slope $\alpha = 0.054 \text{ mm s}^{-1} \text{ \AA}^{-3}$. The approach allows for an accurate estimation of the IS of any Eu compound in a way which is unbiased by nuclear modeling, and has been

tested on the two multivalence systems Eu_3S_4 and Eu_2SiN_3 , for which it gives excellent results. By using the value of α , we also calculated the nuclear parameter $\Delta R/R = 6 \times 10^{-5}$.

For the present case of $\text{Y}_2\text{O}_3:\text{Eu}$ we derive an IS of $+1.04 \text{ mm s}^{-1}$ at the $24d$ site and $+1.00 \text{ mm s}^{-1}$ at the $8b$ site. These values are compatible with experiments, although the experimental estimation of the IS difference is difficult to resolve and depends critically on the fitting procedure.

Acknowledgments

We wish to thank J K Dewhurst and S Sharma for useful discussions and for developing the elk code. This work is dedicated to the memory of our friend and mentor Prof. Sandro Massidda.

Data availability statement

The data that support the findings of this study are available upon reasonable request from the authors.

ORCID iDs

Arkadiy Davydov  <https://orcid.org/0000-0001-6899-5727>
Antonio Sanna  <https://orcid.org/0000-0001-6114-9552>
Giorgio Concas  <https://orcid.org/0000-0003-3422-1066>

References

- [1] Blasse G and Grabmaier B C 1994 *Luminescent Materials* (Berlin: Springer)
- [2] Konrad A, Fries T, Gahn A, Kummer F, Herr U, Tidecks R and Samwer K 1999 *J. Appl. Phys.* **86** 3129
- [3] Schmechel R et al 2001 *J. Appl. Phys.* **89** 1679
- [4] Stanek C R, McClellan K J, Uberuaga B P, Sickafus K E, Levy M R and Grimes R W 2007 *Phys. Rev. B* **75** 134101
- [5] Grill A and Schieber M 1970 *Phys. Rev. B* **1** 2241
- [6] Kern S and Kostecky R 1971 *J. Appl. Phys.* **42** 1773
- [7] Antic B, Mitric M and Rodic D 1997 *J. Phys.: Condens. Matter.* **9** 365
- [8] Concas G, Spano G, Bettinelli M and Speghina A 2003 *Z. Naturforsch. A* **58** 551
- [9] Hohenberg P and Kohn W 1964 *Phys. Rev.* **136** B864
- [10] Kohn W and Sham L J 1965 *Phys. Rev.* **140** A1133
- [11] Singh D J and Nordström L 2005 *Planewaves, Pseudopotentials, and the LAPW Method* (Berlin: Springer)
- [12] Dewhurst J K 2021 The Elk FP-LAPW code <http://elk.sourceforge.net>
- [13] Anisimov V I, Zaanen J and Andersen O K 1991 *Phys. Rev. B* **44** 943
- [14] Concas G, Dewhurst J K, Sanna A, Sharma S and Massidda S 2011 *Phys. Rev. B* **84** 014427
- [15] Monkhorst H J and Pack J D 1976 *Phys. Rev. B* **13** 5188
- [16] Freeman A J and Ellis D E 1978 *Mössbauer Isomer Shifts* (Amsterdam: North-Holland) p 111
- [17] Hanic F, Hartmanova M, Knab G G, Urusovskaya A A and Bagdasarov K S 1984 *Acta Crystallogr. B* **40** 2
- [18] Wyckoff R W G 1964 *Crystal Structures* vol 2 (New York: Interscience Wiley-Interscience)
- [19] Dreizler R M and Gross E 1990 *Density Functional Theory* (Berlin: Springer)
- [20] Hedin L 1965 *Phys. Rev.* **139** A796
- [21] Aryasetiawan F and Gunnarsson O 1998 *Rep. Prog. Phys.* **61** 237
- [22] Tomiki T, Tamashiro J, Tanahara Y, Yamada A, Fukutani H, Miyahara T, Kato H, Shin S and Ishigame M 1986 *J. Phys. Soc. Japan* **55** 4543
- [23] Sharma S, Dewhurst J K, Sanna A and Gross E K U 2011 *Phys. Rev. Lett.* **107** 186401
- [24] Runge E and Gross E 1984 *Phys. Rev. Lett.* **52** 997
- [25] Petersilka M, Gossmann U J and Gross E K U 1996 *Phys. Rev. Lett.* **76** 1212
- [26] Robindro Singh L, Ningthoujam R S, Sudarsan V, Srivastava I, Dorendrajit Singh S, Dey G K and Kulshreshtha S K 2008 *Nanotechnology* **19** 055201
- [27] Shenoy G K 1984 Mössbauer-effect isomer shifts *Mössbauer Spectroscopy Applied to Inorganic Chemistry* ed G J Long (Berlin: Springer) pp 57–76
- [28] Grandjean F and Long G J 1989 Mössbauer spectroscopy of europium-containing compounds *Mössbauer Spectroscopy Applied to Inorganic Chemistry* ed G J Long and F Grandjean (Berlin: Springer) pp 513–97
- [29] Atzmony U, Bauminger E R, Nowik I, Ofer S and Wernick J H 1967 *Phys. Rev.* **156** 262
- [30] Morin D 2008 *Introduction to Classical Mechanics: With Problems and Solutions* (Cambridge: Cambridge University Press)
- [31] Concas G, Muntoni C, Spano G, Bettinelli M and Speghini A 2001 *Z. Naturforsch. A* **56** 267
- [32] Antonov V N, Harmon B N and Yaresko A N 2005 *Phys. Rev. B* **72** 085119
- [33] Görlich E, Hryniewicz H U, Kmiec R, Latka K and Tomala K 1974 *Phys. Status Solidi b* **64** K147
- [34] Zeuner M, Pagano S, Matthes P, Bichler D, Johrendt D, Harmening T, Pöttgen R and Schnick W 2009 *J. Am. Chem. Soc.* **131** 11242